Investigation of the α-cluster structure of ^{22}Ne and ^{22}Mg

V. Z. Goldberg,[1,2,3] G. V. Rogachev,[1] W. H. Trzaska,[4] J. J. Kolata,[1] A. Andreyev,[5] C. Angulo,[6] M. J. G. Borge,[7] S. Cherubini,[6] G. Chubarian,[3,8] G. Crowley,[9] P. Van Duppen,[5] M. Gorska,[5] M. Gulino,[5] M. Huyse,[5] P. Jesinger,[10] K.-M. Källman,[11] M. Lattuada,[12] T. Lönnroth,[11] M. Mutterer,[10] R. Raabe,[5] S. Romano,[12] M. V. Rozhkov,[2] B. B. Skorodumov,[2] C. Spitaleri,[12] O. Tengblad,[7] and A. Tumino[12]

[1]*Physics Department, University of Notre Dame, Notre Dame, Indiana 46556, USA*
[2]*Russian Research Centre "Kurchatov Institute," Moscow, Russia*
[3]*Texas A&M University, College Station, Texas 77843, USA*
[4]*Physics Department, University of Jyväskylä, Jyväskylä, Finland*
[5]*Katholieke Universiteit Leuven, Leuven, Belgium*
[6]*Centre de Recherches du Cyclotron and Institut de Physique Nucléaire, Université catholique de Louvain, B-1348 Louvain-la-Neuve, Belgium*
[7]*Instituto de Estructura de la Materia, Madrid, Spain*
[8]*Joint Institute of Nuclear Research, Dubna, Russia*
[9]*University of South Carolina, Columbia, South Carolina 29208, USA*
[10]*Darmstadt University of Technology, Darmstadt, Germany*
[11]*Åbo Akademi, Turku, Finland*
[12]*INFN—Laboratori Nazionali del Sud, Catania, Italy*

(Received 10 July 2003; published 10 February 2004)

An excitation function for resonance elastic scattering of α particles on ^{18}O and ^{18}Ne was measured using the method of inverse geometry with a very thick target. Spectroscopic information was obtained for 23 levels in the excitation energy region from 11.9 to 13.7 MeV in ^{22}Ne. Twelve of them are new. General features of α-cluster bands in ^{22}Ne are analyzed in the framework of the potential model with a deep potential well. Predictions for the 11^- level in ^{22}Ne, as well as for the isotopic shift of the cluster levels in ^{22}Mg, are given. Evidence is presented that new perspectives on the study of nuclear structure and nuclear spectroscopy can be obtained in complimentary measurements of α-cluster states in mirror $N \neq Z$ nuclei.

DOI: 10.1103/PhysRevC.69.024602 PACS number(s): 21.10.−k, 24.30.−v, 27.30.+t

I. INTRODUCTION

Knowledge of α-cluster structure is mainly based on investigations of light $N=Z$ nuclei [1,2]. The most detailed investigations of α-cluster structure in the ^{16}O and ^{20}Ne nuclei were the result of long-term studies of elastic resonance scattering of α particles on ^{12}C and ^{16}O targets [3–6]. A very clear and beautiful picture of quasirotational bands of levels with large α-particle reduced widths was found in these nuclei, which manifested a molecular structure of cluster levels. The data on ^{20}Ne have been reviewed by Richards [7], who grouped the levels into several cluster bands. It was shown that the 0^- band was characterized by an extremely large reduced width for α decay to the ground state of ^{16}O. Much less is known about α-cluster structure in $N \neq Z$ nuclei. Many theoretical calculations have suggested that clustering remains in systems composed of a collection of α particles and valence nucleons. The most recent results, using the molecular orbital model, can be found in Ref. [8,9] (see also References there). The notion of a "dimer" for a two-center structure and "polymers" for multicenter (chain) states was introduced by von Oertzen. In a series of papers [10–12], he compiled the information on the existence of dimer structures in ^{9}Be and ^{10}Be, as well as the possible existence of further dimers and polymers. He also found a rapid increase of moment of inertia for the dimer states. Older references with similar ideas can be found in Ref. [11].

Investigations of the cluster structures in $N \neq Z$ nuclei have been handicapped by experimental difficulties. Recently, several groups tried to reach cluster states in neutron-rich nuclei by means of radioactive beams. First, Korsheninnikov *et al.* [13] found evidence for states in ^{12}Be with a possible $\alpha+4n+\alpha$ structure. More recently, evidence for similar structures were found in ^{12}Be [14] and ^{10}Be [15]. These very interesting results, with only a few tentative spin determinations, do not yet lead to a clear picture but are rather evidence of the interest in the problem.

In summary, the little information (both theoretical and experimental) that is so far available on molecularlike structures in $N \neq Z$ nuclei is related to the neutron-rich side ($N > Z$) (mainly the heavy isotopes of Be and C). No information is available on these exotic structures in nuclei with a proton excess. There is no clear understanding of what will happen to cluster structure when valence protons are substituted for valence neutrons.

The study of non-self-conjugate nuclei has an advantage in that one can investigate isobaric analog states in mirror systems. Comparison of the results for both systems can bring new spectroscopic information and shed light on such properties as the radii of the cluster states. The thick target inverse kinematics method [16,17] gives the possibility to obtain data for mirror nuclei using both conventional and radioactive beams. First results on investigation of ^{22}Ne α-cluster states by means of the thick target inverse kinematics technique were reported in Ref. [18]. The present work concentrates on a detailed comparison of data in the region a few MeV above the α decay threshold in ^{22}Ne with existing data obtained by conventional methods [19,20]. It is well

known that α capture by ^{18}O plays an important role in astrophysics [21]. The lowest levels, which are in question in this work, are positioned about 2 MeV above the threshold for α-particle decay. The extrapolation of the α-particle reduced widths to lower energies can be important, while direct experimental data are scarce.

The present work also presents the first data on the excitation function for resonance scattering of ^{18}Ne on ^{4}He using a radioactive beam of ^{18}Ne.

II. EXPERIMENT

A. Method of inverse geometry with a very thick target

The method of inverse kinematics using a very thick target originally was proposed at the Kurchatov Institute to study the resonance interaction of heavy ions with α particles [16,22]. The main idea is as follows. A beam of heavy ions enters the scattering chamber through a thin foil. The chamber is filled with a target gas (helium for α-scattering experiments), and the pressure of the gas is adjusted so that the beam stops completely before the detectors, which are placed in the forward hemisphere including at 0°. Due to the big difference in energy losses, a light recoil created in an elastic scattering event of the beam particle on the nucleus of the target gas can easily penetrate further through the gas. These recoils are detected by an array of silicon detectors. Due to the fact that elastic scattering kinematics is well defined, it is clear that the energy of the recoil particle in the detector directly corresponds to a given center-of-momentum (c.m.) energy for the reaction. (Inelastic resonance processes can be identified by a time-of-flight method [23,24].) The energy of the beam decreases in the target due to energy loss to ionization, from the maximum (equal to the initial energy of the beam) down to zero. This means that the whole excitation function can be measured in a single run. There are other attractive features of this method. The beam of ^{18}O, for example, is practically free from any admixtures, while it is not possible to obtain a comparably pure ^{18}O target. Of course, there could be small admixtures in the helium gas of the target. However, the α-particle background from these admixtures can be neglected, because all nuclear processes are much less probable in comparison with resonant reactions. The possible admixtures in the helium gas can influence the specific energy loss of heavy ions, though, and should be taken into account in the cross section analysis. An additional important fact is the ease of making measurements at 0°(180°c.m.) where all resonance cross sections are maximal and the potential scattering is minimal. This advantage can be especially important in attempts to study resonances at very low energies (e.g., for astrophysical purposes). In this case, conventional measurements are also desirable near 180° but they are difficult due to the small energy of α particles scattered by a light target. The energy resolution of the method depends on experimental conditions: it is best at 0° (about 40 keV c.m.) for scattering of heavy ions on helium, degrading at larger angles. It is much worse than in the conventional excitation function experiments, but taking into account the other advantages of the method, it is still reasonable to use it in studies of α-cluster states in light nuclei.

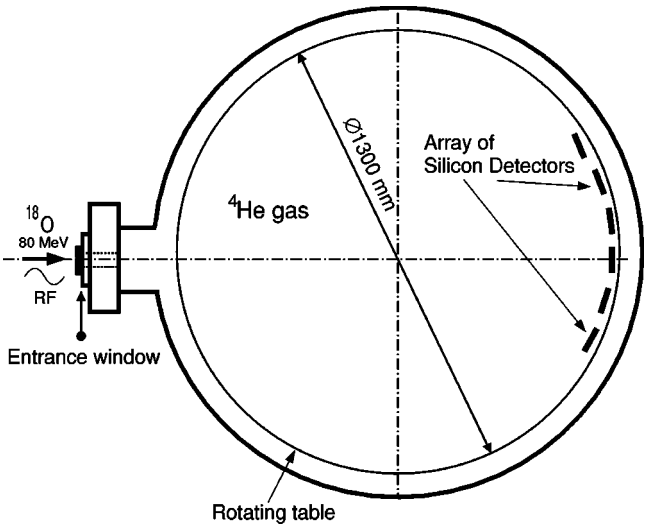

FIG. 1. Experimental setup for the ^{22}Ne experiment.

B. The ^{22}Ne experiment

The experimental investigation of ^{22}Ne was carried out at the K-130 cyclotron of the University of Jyväskylä, Finland, with an 80 MeV ^{18}O beam. The beam entered a large scattering chamber via a 3μm thick Havar window. ^{18}O ions backscattered from this foil were used to monitor the beam intensity. The chamber was filled with helium gas of 99.9% purity at a pressure of 360 Torr. An array of Si detectors positioned in the forward direction was used to detect the recoil α particles. A radio frequency (rf) signal from the cyclotron was used to get time-of-flight information. The experimental setup is sketched in Fig. 1.

C. The ^{22}Mg experiment

The experiment dedicated to the investigation of ^{22}Mg was carried out at the Centre de Recherches du Cyclotron (CRC) at Louvain-la-Neuve, Belgium. A postaccelerated radioactive ^{18}Ne beam having an energy of 53 MeV and an average intensity of 5×10^{5} particles per second was used. The experimental setup was very similar to that used in the investigation of ^{22}Ne. The only significant difference was that in the ^{22}Mg case; due to the lower intensity of the radioactive beam compared to a stable one, we were able to use a microchannel plate detector in front of the scattering chamber (before the entrance window), to detect each particle in the incoming beam. This provided for better time resolution (compared with the rf signal) and for better control of the beam intensity. Improved timing allows for a more clear separation between elastic scattering and all other processes as discussed in Ref. [23].

A short run was also made with a set of thin Mylar foils positioned in the helium gas. The dips in the α-particle spectrum, related to the foils, were used to check the calculations of the ^{18}Ne energy loss in the gas.

III. ANALYSIS AND RESULTS

A. ^{22}Ne

Excitation functions for elastic scattering of α particles on ^{18}O at 20 different angles were measured in the excitation-

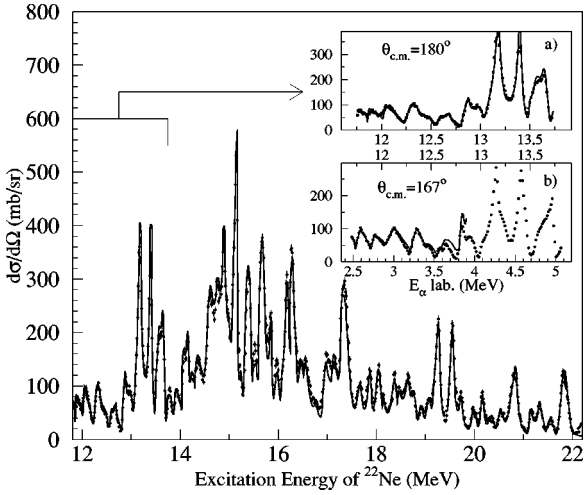

FIG. 2. Excitation functions for elastic scattering of α particles on ^{18}O measured at 0° in lab system (180°c.m.). Inset (b) shows data from Ref. [20]. Inset (a) shows the corresponding data measured in this work.

energy range from 11.8 to 22.2 MeV. In this work, we mainly consider the low-energy range from 11.8 to 14.0 MeV (c.m.). In this energy region the angular distributions were measured from 180° down to 135° (c.m.). This slightly exceeds the region over which all Legendre polynomials of order higher than two have their first minimum. Except at 0°, the same laboratory angles correspond to different c.m. angles for different regions of excitation energy in our setup. The low-energy part of the excitation function (up to 12.5 MeV) was measured with a step of about 4° c.m. The corresponding low-energy α particles could not reach the detectors at the largest angles, since they stopped in the gas. The high-energy part of the excitation function was measured with a step of about 2° (c.m.). The absolute values of the cross sections were obtained with a precision of 25%, mainly related to the determination of the beam current. The data were normalized to fit low-energy Rutherford scattering; the normalization factor obtained was 1.1. The excitation function measured at 0° laboratory angle is shown in Fig. 2. The inset (b) gives the excitation function reported in Ref. [20] in comparison with the corresponding region of excitation function determined in the present experiment. The continuous lines show the results of the best fits to both works (see below). The difference in the quality of the fits is mainly the effect of taking into account the higher excited states in the present work.

The excitation functions shown in Figs. 2–7 were analyzed according to the method proposed by Hausser *et al.* [25] and Billen [6]. Following the procedure outlined in Ref. [5] and successfully used by the Wisconsin group (see Ref. [26], and references therein), we separated the scattering amplitude into a nonresonant term plus the sum of resonant partial waves. For spinless particles, the scattering amplitude can be written as

$$f(\theta) = f_c(\theta) + \rho(\theta)\exp(i\chi) - \frac{i}{2k}\sum_m (2l_m+1)\frac{\Gamma_{l_m}}{\Gamma} \times[\exp(2i\beta_{l_m}) - 1]\exp[2i(\phi_{l_m} + \omega_l)]P_{l_m}(\cos\theta), \quad (1)$$

where ρ and χ are the background amplitude and phase shift, β_ℓ is a resonant phase shift, ϕ_ℓ is a relative background

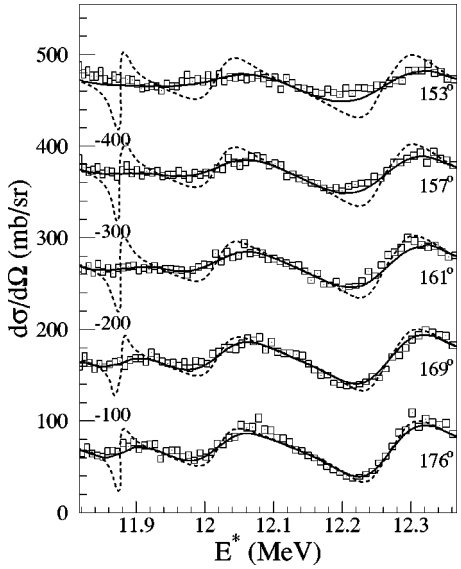

FIG. 3. Excitation functions for elastic scattering of α particles on ^{18}O from 11.76 to 12.36 MeV. Different curves correspond to different detector angles. The solid lines are the convoluted *R*-matrix fit; dashed lines represent the unconvoluted fit. Values under the curve are the bias factors, which were used to create the plot.

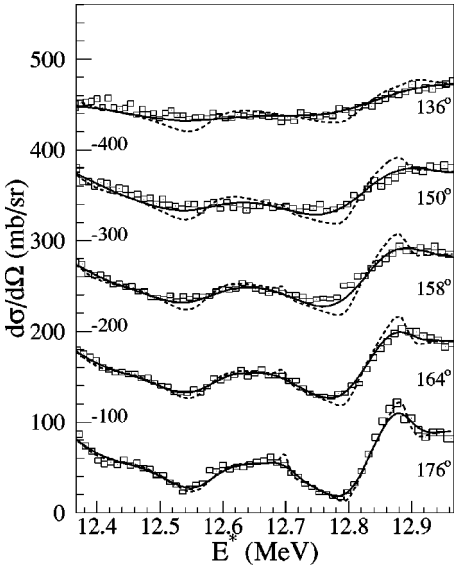

FIG. 4. Excitation functions for elastic scattering of α particles on ^{18}O from 12.36 to 12.96 MeV. Different curves correspond to different detector angles. The solid lines are the convoluted *R*-matrix fits; dashed lines represent the unconvoluted fits. Values under the curve are the bias factors, which were used to create the plot.

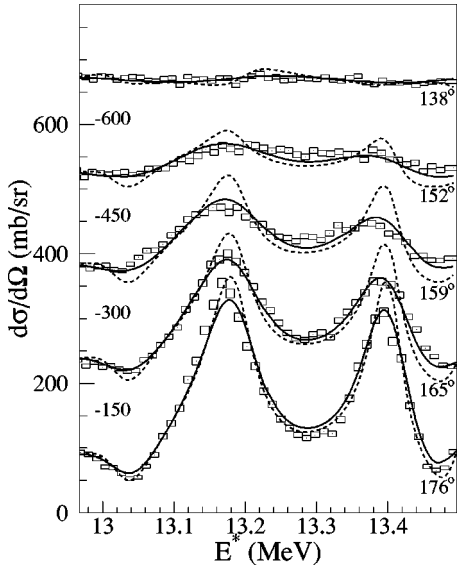

FIG. 5. Excitation functions for elastic scattering of α particles on ^{18}O from 12.96 to 13.46 MeV. Different curves correspond to different detector angles. The solid lines are the convoluted *R*-matrix fits; dashed lines represent the unconvoluted fits. Values under the curve are the bias factors, which were used to create the plot.

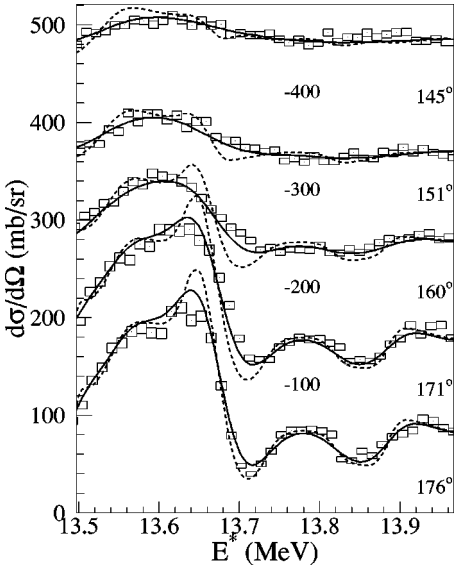

FIG. 7. Excitation functions for elastic scattering of α particles on ^{18}O from 13.5 to 13.96 MeV. Different curves correspond to different detector angles. The solid lines are the convoluted *R*-matrix fits, while dashed lines represent the unconvoluted fits. Values under the curve are the bias factors, which were used to create the plot.

phase shift, and $f_c(\theta)$ and ω_l are the Coulomb amplitude and phase shift. The cross section is given by

$$\frac{d\sigma}{d\Omega} = |f(\theta)|^2. \tag{2}$$

The resonance phase shift is

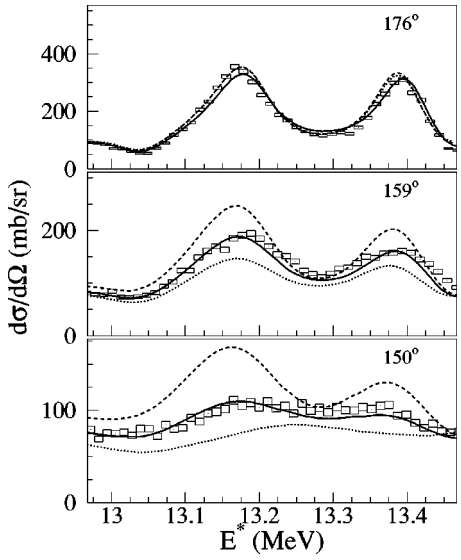

FIG. 6. Excitation function for elastic scattering of α particles on ^{18}O in an energy interval where two strong 3^- levels were observed. The solid curve is the unconvoluted fit with 3^- spin-parity assignment; the dashed and dotted curves show calculations for 2^+ and 4^+ assignments, respectively.

$$\beta_{l_m} = \arctan\left[\frac{\Gamma}{2(E_{res_m} - E)}\right]. \tag{3}$$

The background amplitude ρ was assumed to be smoothly dependent on energy and was interpolated by straight lines connecting a set of energy points (four points for the 4 MeV excitation interval). In order to reduce the number of free parameters, the background phase shift χ was taken to be zero. Phase shifts ϕ_{l_m} were fixed for each resonance and were not varied with angle. It is relatively simple to determine the starting parameters for resonances in the low-energy region. Very often, the width of the resonance is a good indication of the spin. Also it is helpful to know that the phase shift is essentially the Coulomb phase in this low-energy region. The known data [19,20] were used initially only to provide for an approximate position of strong, broad resonances. As a rule, an evident irregularity in the 180° excitation function served as a hint for the presence of a resonance. The best fits, convoluted with the experimental resolution, are shown as solid bold curves in Figs. 2–7. The dashed curves present the nonconvoluted best fit. Table I collects data obtained in the present work and in Refs. [19,20].

B. Resonances between 11.76 and 12.96 MeV

1. The lowest-energy resonance at 11.88 MeV (1^-).

This resonance could be observed at only a few angles in the vicinity of 180°. The anomaly at 180° corresponds to a stronger resonance than reported in Ref. [19,20]. However, the precision of the parameter determination is not certain due to the very high sensitivity of the calculations to the

TABLE I. Parameters of the ^{22}Ne resonances observed in $\alpha + ^{18}$O elastic scattering. Levels at 12.99 MeV and above are from the present experiment. Uncertainties of resonance excitation energies are within 10 keV. See text for details.

Level	E_{exc} (MeV)	J^π	Γ_{tot} (KeV)	$\Gamma_\alpha/\Gamma_{tot}$ (%)	θ_α^2 (%)	Reference
1	11.70	2^+	5	10	1.7	[19]
2	11.76	1^-	11	28	3.1	[19]
	11.76	1^-	11	31	3.1	[20]
3	11.88	1^-	10	56	7	This work
	11.89	1^-	10	36	2.3	[19]
	11.89	1^-	10	34	2.1	[20]
4	12.02	0^+	68	66	28	This work
	12.04	0^+	57	51	8.5	[19]
	12.04	0^+	66	53	9.1	[20]
5	12.25	0^+	76	100	19	This work
	12.26	0^+	74	63	8.9	[19]
	12.26	0^+	66	86	10.3	[20]
6	12.28	1^-	51	10	2	This work
	12.28	1^-	66	10	1.6	[20]
7	12.39	2^+	99	6	5	This work
	12.39	2^+	66	7	1.9	[19]
	12.38	2^+	66	8	2.1	[20]
8	12.57	1^-	105	35	8	This work
	(12.57)	(1^-)	(26)	46	(2.1)	[19]
	12.59	1^-	131	36	6.9	[20]
9	(12.61)	(2^+)	(124)	(4)	3	This work
	(12.61)	(1^-)	(94)	(49)	(7.3)	[19]
	12.61	(2^+)	25	3	0.2	[20]
10	12.70	3^-	15	6	1	This work
11	12.80	2^+	50	12	2	This work
	12.80	2^+	37	11	0.8	[20]
12	12.82	1^-	170	53	12	This work
	12.83	1^-	140	59	8.8	[20]
13	12.89	3^-	39	9	3	This work
	12.88	3^-	45	11	1.9	[20]
14	12.99	0^+	80	40	3	
15	13.03	2^+	90	29	4	
16	13.19	3^-	79	39	13	
17	13.21	0^+	81	39	2	
18	13.40	3^-	58	39	8	
19	13.49	4^+	29	10	5	
20	13.54	0^+	96	77	2	
21	13.57	3^-	136	12	4	
22	13.65	(3^-)	48	16	2	
23	13.67	(2^+)	41	12	<1	
24	13.69	(5^-)	50	4	13	
25	13.73	4^+	57	7	4	
26	13.82	(2^+)	51	7	<1	
27	13.88	4^+	46	7	3	

beam energy spread in the gas. The parameters of the resonance were obtained rather to illustrate possible uncertainties at the end of the investigated region. The influence of the lower-energy resonances on the parameters of the 11.88 MeV resonance was checked. Inclusion of the closest strong 1^- resonance at 11.76 MeV [19,20] has only a minor effect.

2. 0^+ resonances at 12.02 and 12.25 MeV

These strong, broad resonances are evident over a large enough angular interval to reject the 1^- possibility. They are rather close to each other so a formula for two interfering levels with the same spin and parity might be appropriate here. A corresponding analysis [19] showed only small differences in comparison with the simple expression (1); the correction can be taken into consideration by means of small changes of the phase shifts of these resonances using expression (1).

3. 1^- resonances at 12.28, 12.57, and 12.82 MeV

The resonances at 12.57 and 12.82 MeV are strong and were observed over the full angular interval of the present measurements. The resonance at 12.28 MeV is weaker and positioned near a strong 0^+ resonance. Its effect is mainly to fill in the minimum at 12.22 MeV. The parameters of this level are obtained with a somewhat worse precision. All three resonances were observed in Ref. [20].

4. 2^+ resonances at 12.39, 12.61, and 12.80 MeV

Relatively small anomalies at 12.39 and 12.61 MeV can be followed practically throughout the total angular interval of these measurements. (At the angles most distant from zero, the anomalies were smeared out due to the worse resolution.) This was considered as an indication for low spin (less than 3). The final identification was made by their detailed angular behavior and by the phase of the best fit. The resonance parameters agree with previous work [19,20]. The resonance at 12.80 is close to the minimum of the strong 1^- (12.82 MeV) state. There is no evident manifestation of the 12.80 MeV resonance found in Ref. [20] in our data. After inclusion of the resonance, however, the fit to the minimum near 12.8 MeV was improved. The specific parameters of the resonance are the result of this best fit procedure.

5. Other 2^+ resonances

Two additional 2^+ levels were claimed in Refs. [19,20]. The inclusion of the 11.92 MeV resonance, with a tentative 2^+ assignment [19,20], slightly deteriorated the fit. The change of the resonance spin to 1^- slightly improves the fit. The inclusion of the 12.48 resonance, with a tentative 2^+ assignment [20], slightly improves the fit. However, the effects were too small to make definite conclusions in either case.

6. 3^- resonances

A sharp 3^- state is found at 12.89 MeV in agreement with the analysis of Ref. [20]. The total, previously investigated,

region between 11.8 and 13.0 MeV was thoroughly checked for resonances which could have been missed before. The continuous 180° excitation function measured in this experiment gives a basis for a search of this kind. No new structures were found, apart from a hint for a resonance at 12.70 MeV. The inclusion of a narrow 3^- resonance at this energy improved the fit at the top of a broad maximum at 12.68 MeV. The anomaly (if it exists) can be seen at a few angles in the vicinity of 180°.

C. Resonances between 12.96 and 13.46 MeV

The region from 12.96 to 13.46 MeV was studied in only one other work [20]. No conclusions on spin assignments were made due to difficulties of the analysis.

1. 0^+ level at 12.99 MeV

The level manifests itself as a relatively small bump at 180°, and becomes one of the strongest resonances at smaller angles. Its angular behavior makes the spin assignment unambiguous.

2. 2^+ resonance at 13.03 MeV

The level manifests itself as an evident dip at 180° which is present up to extreme angles in this experiment. The phase shift fit and angular distribution give evidence for a spin 2 assignment. However, this level is positioned between two strong resonances (0^+ and 3^-), so that the precision of the parameter determination could be reduced.

3. 3^- resonances at 13.19 and 13.40 MeV

These two resonances are the strongest peaks at 180° in the region in question. Due to interference, they affect all excitation functions at angles where these levels dominate. Figure 6 gives examples of the description of the region of the 3^- resonances at different angles, including the minimum of the Legendre polynomial of order three. The comparison with fits corresponding to assumptions of other spins for these two states (2 or 4) are also given. To make the comparison, the 180° excitation function was fitted under assumptions that the dominant resonances correspond to spins 2, 3, or 4. All other resonance parameters were changed to obtain the best fit. In this way, a good fit could be obtained for 180°, and the fit is still rather good at 176° (see Fig. 6) for different spin assumptions. However, it is evident from Fig. 6 that the results are quite different as one moves further from 180°. Even in the limited angular interval of the present work there are evident differences in the fits corresponding to different assumptions for the spin assignments. In addition, the phase shift has the wrong sign for spin 2 or 4 assignments.

4. Two weak resonances: (0^+, 13.21 MeV) and (4^+, 13.49 MeV)

The presence of these resonances is not very evident to an inspection by eye. The 0^+ resonance fills in the minimum between two strong 3^- resonances; without it the minimum is too deep at angles far from 180°. Its inclusion decreases χ^2 by 20% at 180° and by a factor of 2 at 152°. The 4^+ resonance improves the fit to the corresponding minimum at 180°, decreasing χ^2 by a factor of 3. Proof for both resonances can be obtained from the 90° excitation function of Ref. [20], which indicates the presence of even-spin resonances at the energies in question.

D. Resonances between 13.5 and 13.96 MeV

It appears that the broad bump at 13.56 MeV collects several contributing resonances. The most evident contribution is from a zero-spin resonance at 13.54 MeV. Its presence is manifested by the sharp low-energy edge of the bump at 180° (this resonance also dominates at angles far from 180°, providing for a broad maximum). A zero-spin resonance cannot provide for the rather large cross section at 180°, and the general falloff of the cross section from 180° corresponds to a contribution from $L=3$. All other contributing resonances are a result of the detailed fit. Unfortunately, the deterioration of resolution at angles further from 180° results in a smearing out of the sharp and relatively strong 5^- resonance, which otherwise could easily be observed as a minimum at large angles (see the dashed curve in Fig. 7). Hence, the parameters of the resonances in question should be considered as tentative.

IV. COMMENTS ON THE AGREEMENT WITH PREVIOUS EXPERIMENTAL RESULTS

A check of the overall precision is important for this method. There are several factors which can make the present approach less reliable than the conventional resonance scattering measurements. While an accelerator defines the energy of interaction in conventional studies, in this method the energy calibration of each detector is of primary importance. Moreover, the energy deposited in the detectors must be corrected for the energy loss of recoils in the gas. The latter, in turn, depends upon calculations of energy loss of the incident heavy ion beam. Therefore, it is clear that many parameters must be controlled during the present measurements and one has to rely on the energy loss data. The effect of energy loss data on the general precision of the excitation energy determination depends upon experimental conditions. The closer the beam stops to a detector, the greater the influence is on the low-energy part of the spectrum. Under our experimental conditions, a systematic 7% error in the energy loss data would result in 30 keV errors in the excitation energy for the lowest states, while uncertainties in all other parameters would not exceed 20 keV. As can be seen in Table I, the average difference between the present data and the existing results [19,20] for ten resonances is 10 keV. The small differences do not show a definite trend. Also, it is worthwhile to note that a direct detailed comparison of the experimental data of the present work with the data of Refs. [19,20] is not possible due to the different experimental approaches. The comparison of the results of the analysis was made, but the analysis of the data in the two cases was different. In particular, it is important to note that in the previous analyses the influence of higher-energy resonances was neglected. Taking all this into account, it seems

reasonable to conclude that the errors of the resonance energies (including the analysis errors) are within 10 keV. We also believe that differences in other resonance parameters are mainly due to the different analysis approach. The values of the absolute cross sections agree within 20%.

V. ^{22}Ne α-CLUSTER LEVELS IN THE FRAMEWORK OF THE LOCAL POTENTIAL MODEL AND THE DISCUSSION OF THE ^{22}Ne RESULTS

Large α-particle reduced widths are the main basis to use a potential model for the description of α-cluster states. In the case of a two-body interaction of an α particle with a core, the Pauli principle should be naturally taken into account. This can be accomplished phenomenologically by introducing a repulsion at small interaction distances, directly specifying the surface character of the interaction [27,28]. It can also be carried out by using a deep interaction potential [29,30]. The deeply bound states in this potential are very similar to the states forbidden by the Pauli principle.

The physical state wave functions should satisfy the Wildermuth condition, i.e., the assumption that the α cluster is made of valence nucleons whose quantum numbers with respect to the core must correspond to nucleon orbitals above the Fermi surface of the core nucleons. Thus $\Sigma 2n_i+\ell_i=2N+L$, where n_i and ℓ_i are the node numbers and the angular momenta of the nucleons, which constitute the α cluster, and N and L are the same quantities for the cluster as a whole. In reality, the single-particle structure of the nucleons in the cluster is not obvious, so the core structure determines the minimal value of N. For the $\alpha+^{16}$O system, the minimal value for the sum $\Sigma 2n_i+l_i$ is 8, due to the known shell closure in ^{16}O. This gives four nodes for $L=0$ wave functions. For the ^{22}Ne states in question at excitation energies above 12 MeV, we used wave functions with five nodes for $L=0$ or 1. The number of nodes for other orbital momenta was calculated in accordance with the Wildermuth condition. Rather routine parameters of the Woods-Saxon potential ($R=1.25\times 18^{1/3}$ fm and $a=0.63$ fm) were used. The fit to the centers of gravity of the 0^+ and 1^- states resulted in the depth of the potential, -138.7 MeV and -162 MeV, correspondingly. This potential is similar to the one obtained in Ref. [31], where discrete ambiguities in nuclear optical potentials were resolved for elastic scattering of α particles.

Figure 8 presents the excitation energies for negative parity states together with the potential model calculations. As can be seen, the potential model with the same parameters describes the positions of the higher members of the negative parity band quite well. The potential approach also gives a sum rule for the widths of groups of α-cluster levels with the same spin value. The θ_α column of Table I gives the ratio of α-particle widths of the levels to the single-particle limit. The latter were the widths of α single-particle states generated by the potential approach. The positions of the generated states were fitted to the experimental ones by adjusting the depth of the potential well. This approach gives a more reliable estimation of the single-particle width than the conventional Wigner limit used in Refs. [19,20]. For example, the reduced widths of the 1^- (5.79 MeV) and 3^- (7.16 MeV)

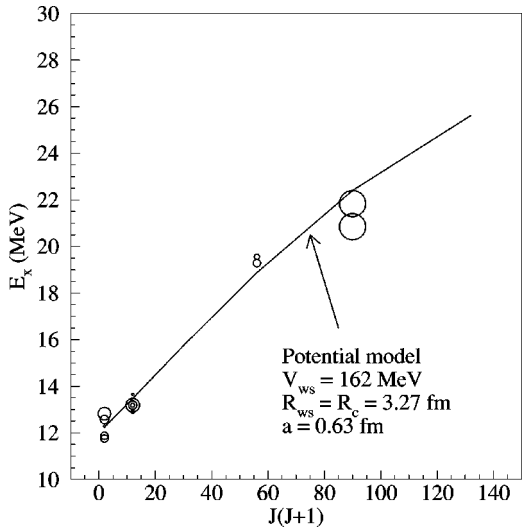

FIG. 8. Energies of negative parity states, together with the potential model calculations. The diameter of the points representing the resonances is proportional to the ratio of reduced α width to the single-particle width. The diameter of the points for 9− resonances was scaled down by a factor of 4.

states in ^{20}Ne will be about 0.9 of the single-particle width generated by the similar potential, while these states are classical examples of pure α-cluster states.

As can be seen from Table I, the 0^+, 1^-, and 3^- states in ^{22}Ne exhaust about 1/3 of the single-particle limit, giving credit to the cluster structure of the states in question as well as to the value of the width limit. The comparison of the values of θ_α obtained earlier [19,20] and those from this work, show clear differences in the absolute values of θ_α, while the experimental data on Γ_α (which is the product of the width of the state on $\Gamma_\alpha/\Gamma_{tot}$ ratio) agree rather well. These differences are the result of the different choice for the single-particle limit and of the choice of a larger radius to calculate the Coulomb wave functions in Refs. [19,20]. The relative values of θ_α generally agree much better except for the case of two 0^+ resonances at 12.0 and 12.3 MeV. For these states our analysis gives a larger θ_α for the 12.0 MeV state, while the previous data [19,20] gave a larger θ_α for 12.3 MeV level. This is a result of the influence of the nuclear potential.

Considering the values of the reduced widths, it is worthwhile to note that the single-particle values, used in this work, are obtained with a "reasonable" cluster potential. The effects of antisymmetrization and the specific behavior of the cluster wave function were taken into account. However, we assumed that the potential parameters are the same for all states in the cluster band. It is known that the well depth of the phenomenological optical potential depends upon energy [31]. While the specific predictions of the microscopic approaches are absent in this case, the uncertainty of the single-particle width can be obtained using the known variation of the parameters of the optical potential for the elastic scattering of α particles (see Refs. [3,31]). As a rule, the well depth parameters are within the interval 140–180 MeV. The well depth variation can be compensated by the radius variation to keep the energy of the generated states unchanged. Radius

variation in its turn influences the single-particle limit. Taking the corresponding changes ($\approx$0.3 fm) of the potential radius into account, the uncertainty of the single-particle widths (and the reduced widths) for the low-spin (broad) states is 20%, and for high-spin (narrow) states can be up to 70%.

It was claimed in Ref. [18] that the dominant α-cluster strength is concentrated in doublets of levels with the same spin value. The present results on low-spin states do not contradict this conclusion. However, taking into account all available states with the same spin one finds that there is some spread of the reduced widths over a few states. Figure 8 presents a distribution of experimental reduced α-cluster widths (as a ratio to the single-particle width) for the 1^- and 3^- states. It can be seen there that a few levels within a 1 MeV energy region exhaust over 30% of the single-particle limit. There are no strong 1^- or 3^- states at higher excitation energy, near the region in question. If there are any 1^- and 3^- states at higher energy, they cannot have substantial reduced α-cluster widths due to the rapid increase in penetrability factors. The number of observed states with the same spin is close to the number evaluated from predictions of statistical models. If one assumes that the spread can be related to a mixture of a cluster state with the continuum states, the matrix element of the mixture would be about 0.5 MeV. A better understanding of this situation could result in the prediction of the α-cluster widths of the resonances near the threshold for α decay. Also it seems very important to find the next member of the band, that is, the 11^- state(s), predicted at about 25 MeV excitation energy in ^{22}Ne. The observation of this state will be very important to check the idea of the doubling of α-cluster levels in ^{22}Ne [18], as well as to confirm the ideas of the potential approach to the description of α-cluster states.

There are no data on high-spin states for the positive parity α-cluster band. Two strong 0^+ low-lying resonances, together with new 0^+ resonances with smaller reduced widths, exhaust more than half of the width. It is not possible to fit the position of the 0^+ resonances with the values of the potential parameters found for the negative parity band. Keeping the same number of nodes in the wave function, one needs to decrease the depth of the potential well by 15% to -138.7 MeV. If we take the number of nodes equal to 6, the required changes are somewhat bigger. The relative positions and widths of low-spin members of the band are weakly dependent upon this choice. It is known for ^{16}O and ^{20}Ne [7] that the degree of clusterization is smaller for the positive parity states, and the need to change the potential to describe both positive and negative parity α-cluster bands in other light nuclei is also known [32]. Therefore, more data on the higher members of the positive parity band are needed to specify the features of this band in ^{22}Ne.

The ^{18}Ne+α data

The spectrum of states in ^{22}Mg should be identical to that in ^{22}Ne if one neglects the Coulomb interaction. It is clear that the Coulomb interaction increases the mass of ^{22}Mg relative to ^{22}Ne. In the same way, the levels in ^{22}Mg are moved up relative to ^{18}Ne+α, and that is the main reason for the 1.5 MeV difference in the thresholds for the α decay in ^{22}Mg and ^{22}Ne (the threshold being lower in ^{22}Mg). There is an even greater difference between the threshold for proton decay in ^{22}Mg and the mirror neutron decay in ^{22}Ne. In ^{22}Ne, the α decay threshold is the lowest, while in ^{22}Mg the threshold for proton decay is 2.6 MeV lower than the α decay threshold. These factors can influence the similarity which would otherwise be expected for the excitation functions of elastic scattering of α particles on ^{18}Ne and ^{18}O. Figure 9 gives both excitation functions in comparison. It is rather evident from Fig. 9 that the dominating doublet in ^{22}Ne is not present in the ^{22}Mg spectrum (its expected position in the $\alpha+^{18}$Ne spectrum is indicated by the arrow).

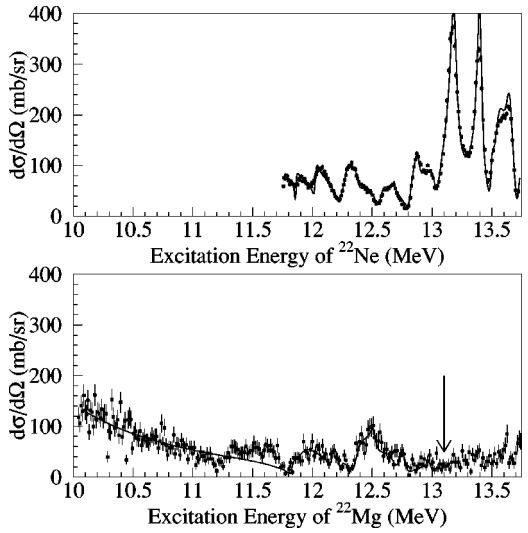

FIG. 9. Excitation functions for $\alpha+^{18}$O (top) and $\alpha+^{18}$Ne (bottom). The arrow on the bottom panel points to the expected excitation energy of the strong 3^- doublet, observed in the ^{22}Ne spectrum.

The quality of the ^{22}Mg data is not sufficient to make an independent analysis of these data. Therefore, the following procedure of analysis was chosen. We assume that the levels with the same spins define the excitation functions of elastic scattering of ^{18}O+α in the region from 11.8 up to 12.9 MeV, and of elastic scattering of ^{18}Ne+α in the region with the approximate borders from 11.8 up to 13.0 MeV. Naturally, the basis for this assumption is the isobaric invariance of nuclear forces and the fact that the resonances in ^{22}Ne in the energy region in question were studied in three experiments (the present work and Refs. [19,20]). Therefore one does not expect a new strong resonance in the ^{22}Mg spectra which has not previously been evident in the ^{22}Ne spectra. The opposite case is possible. Due to the larger number of open channels for nucleon decay in ^{22}Mg some resonances found in ^{18}O $+\alpha$ scattering may not be evident in the ^{18}Ne+α interaction. As can be seen in Fig. 9, a good fit to the part of the ^{18}Ne $+\alpha$ excitation function can be obtained in this way. This fit to the single-angle data is not unambiguous because the total width and the resonance strength cannot be taken from the ^{22}Ne data. More reliable data can be obtained on the resonance energies. The tentative spin assignments for low-spin resonances are given in Table II. We compared the relative positions of the resonances found in ^{22}Mg with the positions

TABLE II. Tentative spin assignment for ^{22}Mg levels.

Level	Spin	Energy (MeV)
1	2	2.87
2	2	3.055
3	0	3.18
4	1	3.32
5	2	3.656
6	1	3.70
7	0	3.76
8	1	4.02
9	0	4.021
10	2	4.085
11	1	4.22

of their mirror states in ^{22}Ne. The level shift averaged over seven resonances appears to be 1.20 ± 0.14 MeV. While this value, as well as the shift for each resonance, can be influenced by taking account of resonances outside the region under consideration, this influence should be much smaller than the quoted error. Therefore, it seems worthwhile to use the value of the average level shift to check the potential model. Figure 10 gives the values of the Coulomb shift which should be observed for the negative parity cluster levels in ^{22}Mg. As can be seen here, the Coulomb shifts of the ^{22}Mg levels relative to the mirror α-cluster states in ^{22}Ne are dependent upon the spin of the state. Levels with different spins (mainly 0^+, 1^-, and 2^+) contribute to the excitation region in ^{22}Mg which is being analyzed. The calculations in the framework of the potential model, with the parameters fixed for the negative and positive parity states in ^{22}Ne, showed that the Coulomb shift for 1^- states is between that for 0^+ and 2^+ states. Therefore the result found for the group of states in ^{22}Mg can be compared with the calculations for the 1^- level, as shown in Fig. 10. The data point in Fig. 10 corresponds to the estimated average energy shift for the states, obtained by the subtraction of decay energies of levels in ^{22}Ne from decay energies of corresponding states in ^{22}Mg (0^+, 1^-, and 2^+ states were used). The calculations agree reasonably well with the observed shift. Simultaneously, this shift, as well as the potential model prediction, is less than the Coulomb difference coming from the values of the thresholds for α decay in ^{22}Mg and in ^{22}Ne. The shift of the structures can be seen even by eye in Fig. 9. In this regard, it seems interesting to consider the main factors affecting the values of the Coulomb shifts as calculated in the framework of the potential model. It was found that reasonable ($\approx$20%) variations of the potential parameters (including changes of rc) result in only relatively small ($\leqslant$200 keV) variations in the Coulomb shifts.

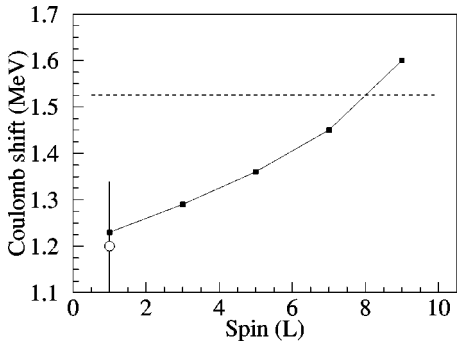

FIG. 10. Energy shift induced by the Coulomb interaction between ^{22}Mg and ^{22}Ne cluster levels, relative to the threshold for α decay. The dashed line shows the difference between the thresholds for α decay in ^{22}Ne and ^{22}Mg. Data point (open circle with the error bars) represents the average experimental value of the energy shift for the states, obtained by subtraction of decay energies of ^{22}Ne states from the decay energies of corresponding states in ^{22}Mg.

The main factor which defines the dependence of the Coulomb shifts upon the spin of a state is the number of nodes in its cluster wave function. The higher the spin of the state, the smaller is the number of nodes, down to a single node for the 11^- state in accordance with the Wildermuth condition. The greater the number of nodes, the more the wave function of the state is pushed to the surface of the nucleus. This is the main factor which defines the general behavior of the Coulomb shifts calculated in the framework of the potential model. Therefore, if one can follow the Coulomb shift for several members of a cluster band, it is possible to derive important information about the fundamental features of the cluster wave functions.

Unfortunately, the 3^- doublet is not evident in the ^{22}Mg spectrum. Using the potential model predictions, we can define the expected position of the doublet in the spectrum, shown by the arrow in Fig. 9. As follows from Fig. 9 if the levels of the doublet are present at the predicted place, the cross section for the population of these levels in ^{22}Mg is at least ten times smaller than in ^{22}Ne. The available data are insufficient to specify the reason for the absence of the 3^- doublet in the ^{22}Mg spectrum. To stress the interest in the problem, we note that von Oertzen observed that the molecular configurations can be very sensitive to the Coulomb interaction, and the same should be true for the unusual structure proposed in Ref. [18].

As can be seen in Fig. 9 there are many anomalies in the ^{22}Mg spectrum at lower energies. The corresponding resonances were not observed in the mirror $\alpha + ^{18}$O scattering due to the very small energies of the α particles. Generally speaking, a proper study of $\alpha + ^{18}$Ne can bring information about the states in ^{22}Ne which are very close to the α-particle threshold, and maybe even below it.

VI. SUMMARY

The present study of the resonances in $^{18}\mathrm{O} + \alpha$ elastic scattering gave information on 27 levels in ^{22}Ne. Fifteen new levels were identified and data were obtained on their spins, excitation energies, and widths.

First results were obtained for elastic scattering of ^{18}Ne $+\alpha$. They showed that the 180° excitation function evidently differs from that of the (mirror) $^{18}\mathrm{O} + \alpha$ elastic scattering. The disappearance of the strong 3^- resonances in the ^{22}Mg spectrum cannot be explained at the moment.

In turn, the excitation function of the $^{18}O+\alpha$ elastic scattering differs from that for nearby $N=Z$ nuclei. The low spin states with large reduced α-widths are close to the α-particle decay threshold in all cases. However, the spectrum of these states in ^{22}Ne differs from that in ^{20}Ne or ^{16}O where the states can be classified as members of a few quasirotational bands. The disappearance of an essential part of the α-cluster reduced width in ^{22}Ne is also a mystery. It might be that the data on a larger excitation energy region can shed some light on these problems. An analysis of these data will be presented in another manuscript. However, several general features of the α-cluster bands could be described in the framework of the potential model with a deep well. The potential parameters are similar to the parameters of the real part of the optical potential which describes elastic scattering of low-energy α-particles. The potential model predicts sharp 11^- levels in ^{22}Ne at about 25 MeV excitation energy. It also predicts the Coulomb shift of the mirror levels in ^{22}Mg, which increases with the increase of the spin of the state. The latter prediction can be considered as a specific reason to proceed in the study of α-cluster states using radioactive beams.

The experimental study was made using the thick target inverse kinematics method. A comparison with previous results showed that the method, which scans a large excitation region, is quite reliable even for the excitation region close to threshold for α decay. At present, the thick target and inverse kinematics approach seems to be the only feasible way to study resonance reactions with low intensity radioactive ion beams.

ACKNOWLEDGMENTS

We thank the CRC staff for the production of the ^{18}Ne radioactive beam and for support during the experiment. This work was supported by NSF Grant Nos. PHY99-01133 and PHY02-030099, RFBR Grant No. 00-02-17401, U.S. DOE Grant No. DE-FG03-93ER40773, and European Community-Access to Research Infrastructure action of the Improving Human Potential Programme, Contract No. HPRI-CT-1999-00110.

[1] A. H. Wuosmaa, R. R. Betts, M. Freer, and B. R. Fulton, Annu. Rev. Nucl. Part. Sci. **45**, 89 (1995).
[2] P. A. Butler and W. Nazarewicz, Rev. Mod. Phys. **68**, 349 (1996).
[3] L. L. Ames, Phys. Rev. C **25**, 729 (1982).
[4] J. John, J. P. Aldridge, and R. H. Davis, Phys. Rev. **181**, 1455 (1969).
[5] S. R. Riedhauser, Phys. Rev. C **29**, 1961 (1984).
[6] J. H. Billen, Phys. Rev. C **20**, 1648 (1979).
[7] H. T. Richards, Phys. Rev. C **29**, 276 (1984).
[8] N. Itagaki and S. Okabe, Phys. Rev. C **61**, 044306 (2000).
[9] N. Itagaki, S. Okabe, K. Ikeda, and I. Tanihata, Phys. Rev. C **64**, 014301 (2001).
[10] W. von Oertzen, Z. Phys. A **354**, 37 (1996).
[11] W. von Oertzen, Z. Phys. A **357**, 355 (1997).
[12] W. von Oertzen, Nuovo Cimento Soc. Ital. Fis., A **110A**, 895 (1997).
[13] A. A. Korsheninnikov *et al.*, Phys. Lett. B **343**, 53 (1995).
[14] M. Freer *et al.*, Phys. Rev. Lett. **82**, 1383 (1999).
[15] M. Freer *et al.*, Phys. Rev. C **63**, 034301 (2001).
[16] K. P. Artemov *et al.*, Sov. J. Nucl. Phys. **52**, 408 (1990).
[17] V. Z. Goldberg and A. E. Pakhomov, Phys. At. Nucl. **56**, 1167 (1993).
[18] G. V. Rogachev, V. Z. Goldberg, T. Lönnroth, W. H. Trzaska, S. A. Fayans, K. M. Källman, J. J. Kolata, M. Mutterer, M. V. Rozhkov, and B. B. Skorodumov, Phys. Rev. C **64**, 051302 (2001).
[19] D. Powers, H. T. Bair, J. L. C. Ford, and H. B. Willard, Phys. Rev. **134**, B1234 (1964).
[20] S. Gorodetzky, M. Port, J. Graff, J. M. Thirion, and G. Chouraqui, J. Phys. (Paris) **29**, 271 (1968).
[21] U. Giesen, C. P. Browne, J. Görres, J. G. Ross, M. Wiescher, R. E. Azuma, J. D. King, J. B. Vise, and M. Buckby, Nucl. Phys. **A567**, 146 (1994).
[22] V. Z. Goldberg, in *Clustering Phenomena in Atoms and Nuclei*, edited by M. Brenner, T. Lönnroth, and F. B. Malik (Springer-Verlag, Heidelberg, 1992), Springer Series in Nuclear and Particle Physics Vol. 7, p. 336.
[23] G. V. Rogachev, Ph.D thesis, Russian Research Centre "Kurchatov Institute," 1999.
[24] K. Markenroth *et al.*, Phys. Rev. C **62**, 034308 (2000).
[25] O. Hausser, T. K. Alexander, D. L. Disdier, A. J. Ferguson, A. B. McDonald, and I. S. Towner, Nucl. Phys. **A216**, 617 (1973).
[26] C. A. Davis and R. Abegg, Nucl. Phys. **A571**, 265 (1994).
[27] I. Shimodaya, R. Tamagaki, and H. Tanaka, Prog. Theor. Phys. **27**, 793 (1962).
[28] A. I. Baz, V. I. Goldanskii, V. Z. Goldberg, and J. B. Zeldovich, *Light and Intermediate Nuclei Close to the Drip Line* (Nauka, Moscow, 1972).
[29] S. Saito, Prog. Theor. Phys. **40**, 893 (1960).
[30] V. G. Neudatchin, V. I. Kukulin, V. L. Korotkikh, and V. P. Korennoy, Phys. Lett. **34B**, 581 (1971).
[31] D. A. Goldberg and S. M. Smith, Phys. Rev. Lett. **29**, 500 (1972).
[32] A. Arima, H. Horiuchi, K. Kuboderaand, and N. Takigawa, Adv. Nucl. Phys. **5**, 345 (1972).